

Revisiting Combinatorial Ambiguities at Hadron Colliders with M_{T2}

Philip Baringer, Kyoungchul Kong, Mathew McCaskey, Daniel Noonan

Department of Physics and Astronomy, University of Kansas, Lawrence, KS 66045 USA

E-mail: baringer@ku.edu, kckong@ku.edu, mccaskey@ku.edu, dnoonan@ku.edu

ABSTRACT: We present a method to resolve combinatorial issues in multi-particle final states at hadron colliders. The use of kinematic variables such as M_{T2} and invariant mass significantly reduces combinatorial ambiguities in the signal, but at a cost of losing statistics. We illustrate this idea with gluino pair production leading to 4 jets + \cancel{E}_T in the final state as well as $t\bar{t}$ production in the dilepton channel. Compared to results in recent studies, our method provides greater efficiency with similar purity

KEYWORDS: Beyond Standard Model, Hadronic Colliders, Supersymmetry Phenomenology.

Contents

1. Introduction	1
2. The p_T versus M method	3
3. Improved method	5
3.1 Brief review of M_{T2}	6
3.2 Case without ISR	7
3.3 Uncertainty in particle masses	8
3.4 Dependence on mass spectrum	9
3.5 Effect of ISR	10
4. Application: the b-ℓ ambiguity in the $t\bar{t}$ dilepton channel	11
5. Summary and conclusions	17

1. Introduction

The Tevatron Run II at Fermilab and the recent turn-on of the Large Hadron Collider (LHC) at CERN are beginning to explore the physics of the Terascale. There are sound theoretical reasons to believe that new physics beyond the Standard Model (BSM) is going to be revealed in those experiments. Perhaps the most compelling phenomenological evidence for BSM particles and interactions at the TeV scale is provided by the dark matter problem. It is a tantalizing coincidence that a neutral, weakly interacting massive particle (WIMP) in the TeV range can explain all of the observed dark matter in the Universe. A typical WIMP does not interact in the detector and can only manifest itself as missing energy. The WIMP idea therefore greatly motivates the study of missing energy signatures at the Tevatron and the LHC. Recently, new ideas of various kinematic methods for the determination of masses, spins, and couplings have attracted a lot of interest in missing energy signatures at colliders (see [1–3] for recent reviews). They not only offer methods for the determination of masses and spins but also provide good background rejection and enhance discovery potential.

Unlike lepton colliders, the environment at hadron colliders is much more complex and often make such tasks difficult. One issue more prevalent in hadron colliders is the combinatorial ambiguities in events, especially in events with jets. In general, the event topology at hadron colliders will typically contain a number of jets. Some come from the decays of heavier particles in the signal and others may originate from initial state radiation (ISR).

The problem gets worse due to detector limitations such as finite resolution, inability of distinguishing quarks from anti-quarks, etc. All these jets pose a severe combinatorics problem: which one of the many jets in an event is the correct one to assign to a particular decay?

Some of the existing studies in the literature simply take for granted that the correct jet can be somehow identified. Others select the jet by matching to the true quark jet in the event generator output, which of course is unobservable. The severity of the jet combinatorics problem is rather model dependent and in practice how well it can be dealt with depends on the individual case at hand. For example, if the mass spectrum is relatively broad, one might expect a jet from the decay of a heavier particle to be among the hardest in the event. This information can be used to improve the purity of the sample. Fortunately, there exists a method (the mixed event technique) which should, at least in principle, remove the effects from incorrect jet combinations [4]. This method has been successfully applied to measuring SUSY masses at the SPS1a study point [5] (see [6] for a more recent study). However, this only works statistically and does not discriminate on an event-by-event basis. The existence of invisible particles adds difficulty in resolving combinatorial issues since it prohibits us from reconstructing the whole signal.

Combinatorial issues appear at all different levels of an event (i.e. from ISR, decays of heavier particles, etc.). A general solution to *all* these problems would be very difficult. We may be able to achieve this statistically by relying on a likelihood analysis or matrix element methods [7]. However, this task requires knowledge of new physics which may not be available at the time of discovery. Therefore, it is desirable to find a solution that is model-independent. In fact, some studies on kinematic variables in the literature already indicate that these variables may be useful for mitigating combinatorial difficulties associated with ISR and the signal jets [8, 9]¹.

The ISR (rather than always proving to be an obstacle) can actually be helpful in the study of BSM physics. This has already been demonstrated in several recent studies. In Ref. [15], ISR was shown to make BSM events more prominent by giving pair-produced new-physics states something to recoil against, thus increasing both \cancel{E}_T and H_T . For the M_{T2} variable (defined in Section 3.1 below) [16, 17], it is known that the transverse momentum of ISR makes the kink structure more pronounced (see references in [1]). Usually ISR overestimates the expected end point, which changes depending on the size of the transverse momentum. To make better measurements one needs to understand systematically the effect of ISR as a function of transverse momentum [18–21].

In this paper, we concentrate on combinatorial ambiguities among the particles in the signal. It is important to resolve or mitigate this combinatorial background issue. Solutions can be directly used to improve experimental measurements such as the forward-backward asymmetry in the top quark pair production, the W -helicity, top mass measurements, etc. In terms of BSM, they obviously become more important since most BSM models predict a WIMP candidate which, when produced, will show up as missing transverse momentum in the detector. An appropriate understanding of combinatorics may even be able to reduce SM backgrounds.

¹See [7, 10–14] for different approaches.

In resolving combinatorial ambiguities in signal events, recently Ref. [22] argued that the proposed p_T versus invariant mass method performs better than the well known hemisphere method [23]. This was shown for parton level events without detector effects, backgrounds or ISR. The results in the previous study are quoted in terms of the efficiency and purity of the samples. For the example point taken in [22] (the 3 body decay of 600 GeV gluino (\tilde{g}) into 2 jets and a neutralino ($\tilde{\chi}_1^0$) of 100 GeV), the authors have obtained 91.7% purity and 3.1% efficiency for the diquark system with an invariant mass less than 500 GeV and a transverse momentum greater than 450 GeV.

The purpose of this paper to revisit the proposed method in [22] and improve the obtained efficiency and purity by utilizing the M_{T2} variable in addition to invariant mass. Section 2 begins with a review of the method described in [22]. In Section 3 we propose our new method for resolving combinatorial ambiguities in the context of gluino pair production with 4 jets + \cancel{E}_T in the final state. Following the spirit of Ref. [22] we analyze our method under similar assumptions in order to make a suitable comparison. Then we determine the effectiveness of this method by considering different mass splittings, possible uncertainties in the gluino and neutralino masses, and ISR. Next, in Section 4, we apply the same method to the $t\bar{t}$ dilepton system to resolve the two-fold ambiguity in pairing a b-tagged jet (b) and a lepton (ℓ). Section 5 is reserved for our conclusions.

2. The p_T versus M method

In this section we briefly review the p_T versus M method in Ref. [22]. For the discussion on combinatorial ambiguities at hadron colliders, the authors consider gluino pair production with each gluino decaying to the lightest neutralino and two quarks: $\tilde{g}\tilde{g} \rightarrow qq\bar{q}\bar{q}\tilde{\chi}_1^0\tilde{\chi}_1^0$. All quarks are treated at parton level and the effects of ISR and parton showering are not considered. Following the example used in [22], we consider the off-shell squark case ($m_{\tilde{q}} > m_{\tilde{g}}$) with a gluino mass $m_{\tilde{g}} = 600$ GeV and a neutralino mass $m_{\tilde{\chi}_1^0} = 100$ GeV (the on-shell case is similar).

Without any ISR, we are left with 4 jets in the final state. In order to do any proper analysis, it needs to be determined which of the 3 possible pairings of jets is the correct combination. In Ref. [22], the authors explored the possibility of extracting the correct jet combination using the invariant mass and transverse momentum of each diquark system. They noticed two prominent features. First, they noted the kinematic edge in the diquark invariant mass distribution, which is especially visible for combinations with high p_T . The excess of diquark combinations with an invariant mass larger than the kinematic edge value ($m_{\tilde{g}} - m_{\tilde{\chi}_1^0} = 500$ GeV) must all be incorrect combinations. Second, those combinations which have invariant mass larger than the kinematic edge (which are all incorrect combinations) tail off quickly towards larger diquark p_T . Events below the edge (which are a mixture of correct and incorrect combinations) extend to higher p_T . Therefore, for the events with larger p_T , the ratio of correct to incorrect combinations increases.

To reproduce the results of Ref. [22] we use the MadGraph/MadEvent package [24] to generate a total of 10K events at the LHC with a center of mass energy of 7 TeV. Simulating

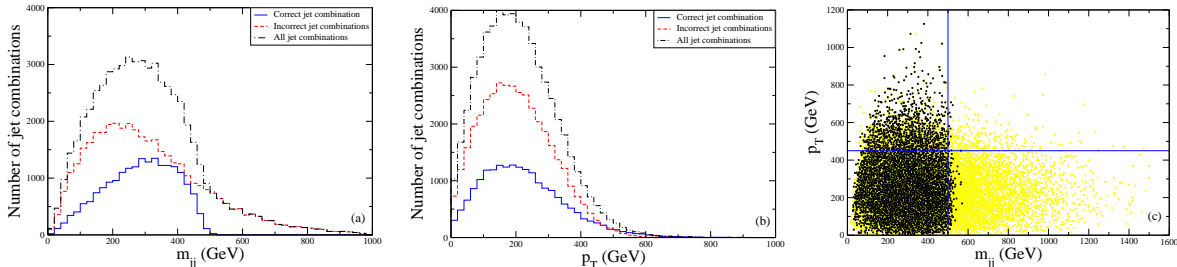


Figure 1: The invariant mass (a) and p_T distributions (b) of the jet combinations in the final state of the gluino pair production. (c) Diquark transverse momentum versus invariant mass for the correct (in black) and incorrect (in yellow) jet combinations. The vertical and horizontal lines represent the cuts used to determine the correct jet combination. These distribution show the motivation for the cuts proposed in [22].

the effects caused by detector resolution in the hadronic calorimeter, the 4-momenta of the final state jets are smeared via

$$\left(\frac{\delta E}{E}\right)^2 = \frac{a^2}{E} + b^2, \quad (2.1)$$

where $a = 0.5$ (0.1) $\sqrt{\text{GeV}}$ and $b = 0.03$ (0.007) for jets (leptons) [23, 25, 26].

Fig. 1 shows (a) the p_T and (b) invariant mass distributions for the correct (blue, solid), incorrect (red, dashed) and all (black, dot-dashed) combinations of jets. The different normalizations of the three histograms are understood since there are two incorrect pairs and one correct pair in each event. In the invariant mass distribution of the correct jet combination there is a clear cutoff at $m_{\tilde{g}} - m_{\tilde{\chi}_1^0} = 500$ GeV. A small fraction of events beyond this kinematic edge occur due to detector resolution. In the p_T distribution at high value ($p_T \gtrsim 500$ GeV) the ratio of correct to incorrect jet combinations becomes $\gtrsim 1$. The p_T cut is chosen such that only 5% of the combinations with an invariant mass above the kinematic edge (which are likely to be incorrect combinations) survive. As suggested, a cut on combinations with the invariant mass below the kinematic edge and above the p_T cut can guarantee an event sample dominated by correct combinations. To extract the correct jet combination the following cuts are made:

- The invariant mass of the diquark pair is less than 500 GeV.
- The p_T of the diquark pair is greater than 450 GeV.

If only one combination of jets passes these cuts then the event is accepted, otherwise the event is discarded. Fig. 1(c) shows the diquark transverse momentum versus invariant mass of the correct (black) and incorrect (yellow) jet combinations. The vertical and horizontal lines represent expected cuts to reduce the number of incorrect combinations. Counting those events that pass two cuts (*i.e.*, the number of events in the left-upper corner of Fig. 1(c)), we find an event efficiency of 3.1% with an event purity of 91.7%. This is consistent with the results in Ref. [22]. Furthermore, a higher efficiency can be achieved at the cost of lower

purity by imposing a lower p_T cut. It is also shown in [22] that this method performs better than the hemisphere method.

3. Improved method

We note that the method discussed in the previous section has a low efficiency while the corresponding purity is relatively high. This is due to the long tail in the p_T distribution of the diquark system. In general, for a large mass splitting between the mother and daughter particles, the p_T of the resulting diquark system is relatively large. Conversely, it is smaller for a narrower spectrum, *i.e.*, the peak position in the p_T distribution is shifted to a lower value in a narrower mass spectrum. Therefore there is a correlation between the location of the peak in the distribution and the mass difference. However the amount of shift (or the location of the peak) is not well enough predicted quantitatively for this observation to be useful, since the diquark system inherits some kinematic information of the mother particles at the production level. An ISR jet is also problematic since the mother particle system will be boosted in the opposite direction of the ISR resulting in modification of the p_T spectra. Unlike the invariant mass distribution, the p_T distribution does not exhibit any kinematic edge. The distribution of the background (incorrect combinations) has a similar shape and, as argued, it decreases faster than the distribution of the correct combination above a certain value (Fig. 1(b)). On the other hand, the invariant mass distribution shows a clear kinematic edge in the distribution of the correct combination but not in that of the incorrect combination, making the two distributions distinct (Fig. 1(a)).

One can recall a similar situation in the leptonic decay of the W boson at hadron colliders. The mass of the W boson in principle can be measured from the p_T distribution of a decay product (a lepton). It shows a nice kinematic edge at half of the W mass when the W boson is produced at rest. However, in reality the transverse mass is used instead. It shows a kinematic edge at the mass of the W and the value of the end point is stable under the presence of initial state radiation. What variable would do such a job for the example in the previous section while increasing the event efficiency? In this paper, instead of cutting on p_T , we propose to use M_{T2} as the second cut in addition to the invariant mass. It is the most natural extension of the transverse mass in the final state when more than one missing particle is present. As advertised, it shows a clear kinematic edge and is stable (*i.e.*, keeping the end point at the same value) under a boost of the whole system. One should investigate how well it performs in terms of the event efficiency and purity.

We consider the same process (4 jets and 2 neutralinos) as in the previous section without any ISR and discuss a method to improve the event efficiency and purity. Then, we discuss how our results change with different mass spectra and the effect of uncertainty in mass measurements. Finally, we look at the same process with ISR and discuss how our results change if we are correctly able to identify the ISR jet. First, we begin this section with a review of M_{T2} .

3.1 Brief review of M_{T2}

The traditional M_{T2} variable is defined as follows [16, 17]. Consider a pair production of a mother particle, P , and their decays down to a daughter particle of mass M_d . For any given event, one can construct the transverse mass, M_{iT} , of each parent:

$$M_{iT}^2 \equiv m_i^2 + M_d^2 + 2(E_{iT}E_{iT}^d - \vec{p}_{iT} \cdot \vec{p}_{iT}^d), \quad (3.1)$$

where

$$E_{iT} \equiv \sqrt{m_i^2 + |\vec{p}_{iT}|^2}, \quad E_{iT}^d \equiv \sqrt{M_d^2 + |\vec{p}_{iT}^d|^2}, \quad (3.2)$$

is the transverse energy of the visible particles, V_i , and daughter particle, d , in the decay branch of each mother particle, correspondingly. \vec{p}_{iT} and m_i are the transverse momentum and invariant mass of the visible particles in branch i ($i = 1, 2$). The individual momenta, \vec{p}_{iT}^d , of the missing daughter particles, d , are unknown, but they are constrained by the measured missing transverse momentum, \vec{P}_T , in the event:

$$\vec{p}_{1T}^d + \vec{p}_{2T}^d = \vec{P}_T \equiv -\vec{P}_T - \vec{p}_{1T} - \vec{p}_{2T}. \quad (3.3)$$

Here \vec{P}_T is the Upstream Transverse Momentum (UTM), which is the transverse momentum of all other visible particles that are not considered in the decay chains. For the true values of the missing momenta, \vec{p}_{iT}^d , each transverse mass in Eq. 3.1 is bounded above by the true parent mass, M_P .

This fact can be used in a rather ingenious way to define the Cambridge M_{T2} variable [16, 17]. One takes the larger of the two quantities in Eq. 3.1 and minimizes it over all possible partitions of the unknown daughter momenta, \vec{p}_{iT}^d , subject to the constraint in Eq. 3.3:

$$M_{T2}(\tilde{M}_d, \vec{P}_T, \vec{p}_{iT}) \equiv \min_{\vec{p}_{1T}^d + \vec{p}_{2T}^d = \vec{P}_T} \{ \max \{ M_{1T}, M_{2T} \} \}. \quad (3.4)$$

Since the masses of the mother and daughter particles are not known in advance, one should treat M_{T2} as a function of the trial mass (\tilde{M}_d) of the daughter particle. For a given \vec{P}_T , the endpoint M_{T2}^{max} of this distribution gives the parent mass, \tilde{M}_P , as a function of the input trial daughter mass, \tilde{M}_d . An important property of M_{T2} is

$$\tilde{M}_P(\tilde{M}_d = M_d) = M_{T2}^{max}(\tilde{M}_d = M_d) = M_P. \quad (3.5)$$

Then one is able to obtain a one dimensional relation between two masses. In cases with non-zero UTM and composite visible system, a kink structure appears, allowing simultaneous determination of both masses (see [1] and references therein).

In the case of $\vec{P}_T = 0$, the analytic expression for M_{T2} can be obtained, while for $\vec{P}_T \neq 0$ case there is no analytic solution to minimization and one has to rely on a numerical code for computation. A clever trick to get around this has been proposed in Ref. [20]. The idea is to project further the transverse quantities with respect to the non-zero UTM, in which case the momentum conservation in the direction perpendicular to the UTM is independent of the UTM (by construction) and one is able to use an analytic expression for the computation of projected M_{T2} . M_{T2} has been extended to cases with non-identical mothers [27] and non-identical daughters [28]. In principle, one can use it for an associated production as well as processes with two different daughter particles.

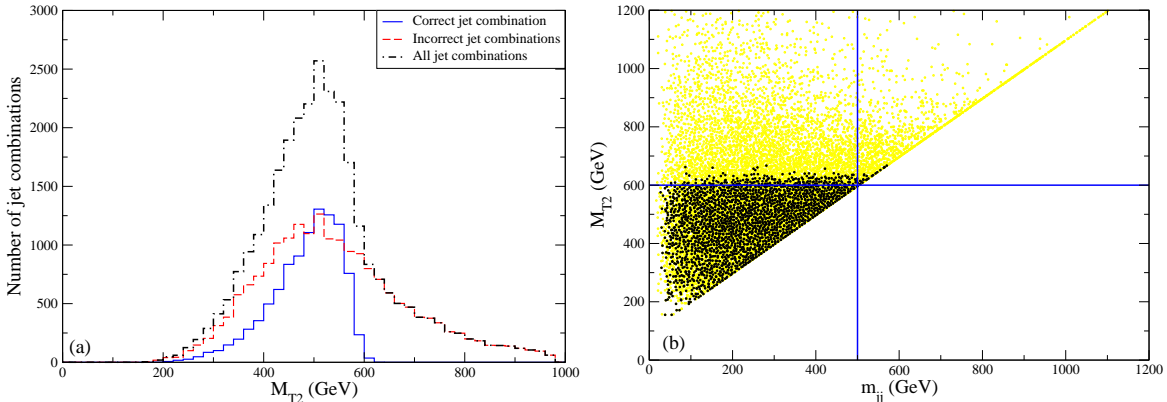


Figure 2: (a) The M_{T2} distribution of the correct and incorrect combinations of jets in the gluino pair production. For the correct jet combination a clear cutoff appears at the gluino mass. (b) The M_{T2} versus invariant mass for the correct (in black) and incorrect (in yellow) jet combinations. The vertical and horizontal lines represent the cuts used to determine the correct jet combination.

3.2 Case without ISR

As an alternative method, instead of using transverse momentum, one uses M_{T2} to help determine the correct jet combination. Fig. 2(a) shows the M_{T2} distribution for the correct (blue, solid), incorrect (red, dashed) and all (black, dot-dashed) combinations of jets. Note that the normalization of the distribution of incorrect (all) pairs is twice (three times) higher than that of the correct distribution. The distribution for the correct jet combination has a clear cutoff at the gluino mass ($m_{\tilde{g}} = 600$ GeV). We apply the same cut that was used in the p_T versus M method for the invariant mass of the jet combinations but now we also require $M_{T2} < 600$ GeV. As before, we keep the events where only one combination of jets passes both cuts. Fig. 2(b) shows the correct (black) and incorrect combinations (yellow) in M_{T2} versus invariant mass. For events where only one combination of jets pass the two cuts, we obtain an event efficiency of 20% with an event purity of 95% as shown in Table 1. Thus we have a concrete example showing that an appropriate choice of kinematic variable cuts enhances both the efficiency and purity of our signal.

Unlike the cuts using p_T , a very small fraction of events with correct combinations are ruled out completely by our cuts (*i.e.*, many events have 2 or 3 combinations that pass the M_{T2} and invariant mass cuts). Table 1 shows the number of events passing our cuts broken down by the number of combinations that pass. With these cuts only 2% of the correct combinations are discarded and 98% of correct combinations survive, so it is possible to use more refined cuts to extract the correct combination from the events with 2 and 3 combinations which could potentially increase the event efficiency even above 20%. In principle, one can apply a p_T cut at this point. However, as argued, p_T is dependent on the mass spectrum and ISR, and perhaps it should be the last variable to make a cut on. Instead, we further increase the efficiency and purity of this procedure by simply taking a look at the events where only two combinations pass the cuts so far.

Number of passed combinations	Number of events	Number of events with correct combination
0	70	–
1	2003	1896
2	3135	3076
3	4792	4792

Table 1: The breakdown of the number of events that have 0 – 3 combinations that pass the M_{T2} and invariant mass cuts. The events with one correct combination give us a 20% (2003/10000) event efficiency with an event purity of 95% (1896/2003). With these cuts only 2% of the correct combinations are discarded so it is possible to use more refined cuts to extract the correct combination from the events with 2 and 3 combinations.

Making further cuts allows us to extract the correct combination from the two that are left over. We discuss two such ways of extracting the correct combination using the invariant mass and M_{T2} distributions. In Figs. 1(a) and 2(a) we can see that for invariant masses and M_{T2} that are below the kinematic cutoff the correct combination tends to be closer to the cutoff than the incorrect combination. We can take advantage of this by introducing a second cutoff. In the case of the M_{T2} distribution we require that one combination have an M_{T2} above this cutoff and the other is below. We then take the combination that is above this cutoff as the correct one. To select the cutoff we maximize the sensitivity ϵD^2 , where the ϵ is the efficiency, $D = 2P - 1$ is the dilution, and P is the purity. This is a commonly used method for optimization in such situations [29]. Fig. 3(a) shows that the maximum sensitivity occurs at an M_{T2} cutoff at 460 GeV which would give us an overall combined efficiency of 33% and purity of 84%. In the case of the invariant mass distribution, each combination has a pair of invariant masses so the cuts need to be modified slightly. From the two jet combinations we take the pair of invariant masses that have the largest separation between them. Placing a cut on the invariant mass we require that one invariant mass is above and the other is below the cutoff. We then take the combination with the invariant mass pair above the cutoff as the correct combination. Fig. 3(b) shows the scan of this invariant mass cutoff. We see that a cutoff of 230 GeV gives the largest sensitivity to this set of events. Combined with the results from the first set of cuts we obtain a total event efficiency of 41% and a purity of 79%.

3.3 Uncertainty in particle masses

Up to this point we have assumed the exact masses of the gluino and the lightest neutralino. What if the masses are not known with absolute certainty? To investigate the effects due to an uncertainty in mass measurements on the event efficiency and purity in finding the correct pairs, we generate events where both the masses of the gluino and neutralino fluctuate by 10%. Then using exactly the same cuts as before ($m_{jj} < 500$ GeV and $M_{T2} < 600$ GeV for all mass spectra) we compute the event efficiency and purity, as shown in Table 2.

A 10% increase in the gluino mass in general increases the invariant mass and M_{T2} of

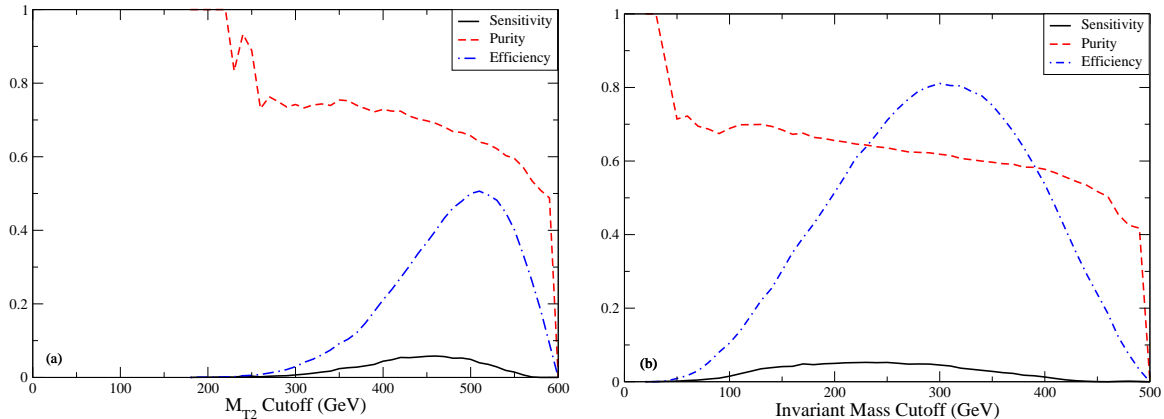


Figure 3: The sensitivity (solid, black), efficiency (blue, dot-dashed) and purity (red, dashed) as functions of the (a) M_{T_2} and (b) invariant mass cutoff. The cutoffs are used to pick the correct combination out of the events where only two combinations passed the original cuts. We see that a M_{T_2} cut (invariant mass cut) of 460 GeV (230 GeV) produces the largest sensitivity. Combining the results of the first set of cuts we have an overall efficiency of 33% and a purity of 84% (41% and a purity of 79%) with additional M_{T_2} cut (invariant mass cut).

the jet pairs, effectively reducing the probability that the jet pair will pass the cuts. In other words, some events with all three combinations surviving cuts end up having only one or two combinations filtered by this variation. This results in an increasing event efficiency, but the contamination lowers the event purity. On the other hand a gluino mass that is 10% smaller decreases the invariant mass and M_{T_2} of the jet pairs, which increases the probability that a jet combination will pass all the cuts. This will lower the event efficiency but will raise the event purity due to the fact that in events with only one combination passing all the cuts, that combination is more likely to be the correct one.

The uncertainty in the neutralino mass produces the opposite effect on the event efficiency and purity. Because the neutralino is a daughter particle, increasing (decreasing) the neutralino mass will increase (decrease) the probability of a jet combination passing our cuts producing the opposite effect to the event efficiency and purity than a similar change in gluino mass. However, it can be seen that the effect on the event efficiency and purity is much milder than that of the gluino due to the smaller change in neutralino mass. Therefore, overestimating the mass of the mother particle (or underestimating the mass of daughter particle) decreases efficiency and increases purity, while underestimating the mother particle mass increases efficiency and decreases purity.

3.4 Dependence on mass spectrum

In principle, this method does not require a large mass splitting between the gluino and neutralino in order to be effective. To quantify this we scan the gluino and neutralino mass over a range of values. Assuming that the gluino and neutralino masses are known, we take

	$m_{\tilde{\chi}_1^0} = 90$	$m_{\tilde{\chi}_1^0} = 100$	$m_{\tilde{\chi}_1^0} = 110$
$m_{\tilde{g}}=660$	0.31/0.61	0.30/0.63	0.28/0.65
$m_{\tilde{g}}=600$	0.21/0.92	0.20/0.95	0.19/0.96
$m_{\tilde{g}}=540$	0.13/1.00	0.12/1.00	0.11/1.00

Table 2: The event efficiency (left) and purity (right) with a 10% uncertainty in the gluino and neutralino masses (in GeV). For all mass spectra the same cuts, $m_{jj} < 500$ GeV and $M_{T2} < 600$ GeV, are applied.

	$m_{\tilde{\chi}_1^0} = 50$	$m_{\tilde{\chi}_1^0} = 100$	$m_{\tilde{\chi}_1^0} = 150$	$m_{\tilde{\chi}_1^0} = 200$	$m_{\tilde{\chi}_1^0} = 250$
$m_{\tilde{g}}=700$	0.15/0.94	0.17/0.94	0.20/0.93	0.22/0.93	0.28/0.93
$m_{\tilde{g}}=600$	0.17/0.95	0.20/0.94	0.24/0.93	0.26/0.93	0.28/0.92
$m_{\tilde{g}}=500$	0.21/0.94	0.24/0.93	0.28/0.93	0.31/0.93	0.36/0.91
$m_{\tilde{g}}=400$	0.25/0.94	0.30/0.93	0.34/0.91	0.37/0.91	0.43/0.87
$m_{\tilde{g}}=300$	0.30/0.93	0.36/0.92	0.42/0.90	0.48/0.85	0.54/0.80

Table 3: The event efficiency (left) and purity (right) for several values of the gluino and neutralino masses (in GeV). For each mass spectrum the invariant mass and M_{T2} cuts are given in Eqs. 3.6 and 3.7.

the following cuts on the invariant mass and M_{T2} :

$$m_{jj} < m_{\tilde{g}} - m_{\tilde{\chi}_1^0}, \quad (3.6)$$

$$M_{T2} < m_{\tilde{g}}. \quad (3.7)$$

The results are summarized in Table 3.

In the increasing $m_{\tilde{g}}$ direction, the invariant mass and M_{T2} distributions of the correct and incorrect jet combinations becomes more spread apart. In general this would increase the chance that a certain jet combination will be cut, reducing the event efficiency. However, the events that survive with only one passed combination will more likely be the correct combination, leading to a larger event purity. In the increasing $m_{\tilde{\chi}_1^0}$ direction, the invariant mass and M_{T2} distributions of the correct and incorrect jet combinations becomes more compressed, resulting in higher efficiency and lower purity.

3.5 Effect of ISR

Since gluino pair production gives a multi-jet final state, it is important to address an issue with isolating ISR jets. The ability to identify ISR is essential for using the discussed procedure: if the jets from ISR are not correctly isolated then it would be impossible to find the correct jet combination. Several different methods have been proposed to identify an ISR jet [7–14]. To analyze the gluino pair production with a single ISR jet we concentrate on the procedure introduced in Ref. [8]. In order to identify the ISR jet we use the following procedure.

1. The jets with the highest momentum are not considered to be the ISR jet and are automatically placed in different gluino decay chains.

Number of passed combinations	Number of events	Number of events with correct combination	Number of events with M_{T2} cut	Number of events with correct combination and M_{T2} cut
0	10	–	17	–
1	454	419	580	533
2	773	754	1103	1083
3	1176	1176	1942	1942
total events	2413	–	3642	–

Table 4: The breakdown of the number of events that have 0-3 combinations that pass the M_{T2} and invariant mass cuts. The correct ISR jet has been identified using the two methods explained in the text. The events with one correct combination give us an event efficiency of 19% and 16% for the events without and with the M_{T2} cutoff respectively. Both sets of events have an event purity of 92%.

2. For the three other jets, each one is taken out and M_{T2} is calculated from all the possible combinations of the remaining jets. The minimum M_{T2} of the possible jet combinations is identified as $M_{T2}^{(i)}$.
3. The jet associated with the minimum of the $M_{T2}^{(i)}$'s is taken to be the ISR jet.

Using this procedure alone we find that the ISR jet can be correctly identified 24% of the time. This number can be improved slightly by putting a minimum cutoff for the M_{T2} of $\min(M_{T2}) > 500$ GeV. In general, if a correct jet is taken out then the resulting M_{T2} becomes much smaller so this minimum M_{T2} cutoff is designed to prevent the small M_{T2} that arises from taking out a hard jet. With this minimum cut included we find that the correct ISR jet can be identified 36% of the time. Both of these numbers are consistent with the results given in Ref. [8]. If we look at the events that have correctly identified the ISR jet and apply the same cuts as before to isolate the correct combination of jets, we can see how our procedure fares with the addition of ISR. The results are given in Table 4. We find that for the events where the ISR was identified without the M_{T2} minimum cutoff, the efficiency of finding the correct combination is 19% with a purity of 92%. Including the minimum M_{T2} cut the efficiency is found to be 16% also with a purity of 92%. Though the efficiency drops slightly there are more events in this group where the correct ISR jet is identified. It is very important to note that these results were obtained from the events where the ISR jet was correctly identified. If we were to include the events where the incorrect ISR jet was identified then our purity will suffer. This exemplifies the importance of correctly identifying the ISR jet in this process.

4. Application: the b - ℓ ambiguity in the $t\bar{t}$ dilepton channel

In this section, we apply the same idea as in Section 3 to resolve the two fold ambiguity that arises in $t\bar{t}$ production in the dilepton channel at the Tevatron and the LHC. Since there

are two leptons associated in this analysis, the corresponding background is already small. Requiring one or two b -tagged jets makes the background negligible. As an illustration, we estimated the cross sections for the signal and SM backgrounds at the 7 TeV LHC. We have used $m_t = 173$ GeV. Assuming the cross sections summarized in Table 5, we simulate the signal ($t\bar{t}$) and background events with PYTHIA [30] and further process them with PGS [31] for detector effects. We require two leptons, at least two jets, and missing transverse energy. The default cuts in each MC event generator are applied along with an extra dilepton invariant mass cut, $40 \text{ GeV} < m_{\ell\ell} < 200 \text{ GeV}$. Table 6 summarizes the number of signal (S) and background (B) events in each channel for zero, one, and two b -tagged jets. The background cross sections are reduced significantly by requiring at least two leptons ($S0/B0 \sim 3.27$) and b -tagging further reduces the backgrounds ($S1/B1 \sim 24$ for one b -tagged jet and $S2/B2 \sim 75$ for two b -tagged jets). Although this conclusion with a naive estimation of the background cross section may be affected slightly due to systematic uncertainties and higher order corrections, we do not expect significantly different results in this two-lepton and one or two b -tagged final state. Therefore we will not address background issues in the rest of this section and will assume the background is negligible.

For the analysis in the rest of this section, we generate 10K $t\bar{t}$ events using the MadGraph/MadEvent package at both the Tevatron and the 7 TeV LHC. We force the W -boson to decay leptonically into either an electron or muon. For events simulated at the LHC, detector resolution was simulated as in Eq. 2.1. For the Tevatron, the detector resolution is simulated following the parametrization in PGS [31],

$$\frac{\delta E}{E} = \frac{0.8}{\sqrt{E}} \quad \text{for jets,} \quad (4.1)$$

$$\frac{\delta E}{E} = \frac{0.2}{\sqrt{E}} + 0.01 \quad \text{for leptons.} \quad (4.2)$$

We also assume that the ISR is correctly isolated. This can be justified given that we require two b -tagged jets for our study on combinatorial issues. To separate the correct and incorrect combinations, we use the same method using the invariant mass of each b - ℓ pairing as well as the M_{T2} variable. The distributions for the correct and incorrect combinations for M_{T2} are shown in Fig. 4 for both Tevatron (in (a)) and LHC (in (b)). The correct combinations have a cutoff at m_{top} , while the incorrect combinations have a tail extending beyond this cutoff. Fig. 5 shows the distributions for $m_{b\ell}$, the invariant mass of the b -jet lepton pairings at the Tevatron (in (a)) and the LHC (in (b)). Both show a kinematic edge at $\sqrt{m_{top}^2 - m_W^2} \approx 153$ GeV.

Specific cut values, $M_{T2} < 176$ GeV and $m_{b\ell} < 156$ GeV, are found by maximizing the sensitivity, defined as $S = \epsilon(2P - 1)^2$. Events are selected if only one of the combinations passes these cuts. The efficiency (ϵ) determines the fraction of $t\bar{t}$ events passing this criterion and the purity (P) is defined as the fraction of lepton-jet pairs that are correctly determined. One can optimize these cuts differently, depending on whether higher purity (but lower efficiency) or higher efficiency (but lower purity) is desired. Table 7 (Table 8) shows the results at the LHC (Tevatron) broken down by the number of combinations that pass the invariant

Process	generator	order	final state	cross section (pb)
$t\bar{t}$	THEORY [32]	NNLL resummation	$t\bar{t}$	163
W^+	FEWZ [33]	NNLO	$\ell^+\nu + \text{jets}$	16670
W^-	FEWZ	NNLO	$\ell^-\bar{\nu} + \text{jets}$	11379
Z/γ^*	MCFM	NLO	$\ell^+\ell^- + \text{jets}$	3000
W^+W^-	MCFM [34]	NLO	inclusive	43
$W^+ + Z/\gamma^*$	MCFM	NLO	inclusive	11.8
$W^- + Z/\gamma^*$	MCFM	NLO	inclusive	6.4
$Z/\gamma^* + Z/\gamma^*$	MCFM	NLO	inclusive	5.9

Table 5: Cross sections for 7 TeV pp collisions. ℓ includes e and μ . $Z/\gamma^* + \text{jets}$ are computed for $40 \text{ GeV} < m_{\ell\ell} < 200 \text{ GeV}$ with default cuts in MCFM.

	B0	S0	B0+S0	B1	S1	B1+S1	B2	S2	B2+S2
e^+e^-	608	990	1598	61	682	743	7	246	253
$e^+\mu^- + e^-\mu^+$	97	2261	2358	6	1534	1540	0	509	509
$\mu^+\mu^-$	663	1220	1883	59	822	881	7	290	297
total	1368	4471	5839	126	3038	3164	14	1045	1059

Table 6: The number of signal (S) and background (B) events in each channel. The numbers (1 and 2) represent the number of b -tagged jets. Applied cuts are nominal reconstruction cuts at PGS level and dilepton invariant mass cut, $40 \text{ GeV} < m_{\ell\ell} < 200 \text{ GeV}$.

mass and M_{T2} cuts in each event. When the restriction that only one combination passes the cuts is applied, we obtain an efficiency of 51.7% (39.9%) and a purity of 94.9% (91.9%).

The CDF collaboration uses several methods to correctly pair the b -jet and the lepton [29]: $m_{b\ell}^{max}$, the kinematic method, and the neutrino phi weighting method. Let us explain each method briefly.

$m_{b\ell}^{max}$ method: Since there are two leptons and two b -jets in each event, there are two exclusive pairing options so there are in total four $m_{b\ell}^2$ values. One takes the pairing option having the maximum $m_{b\ell}^2$ as the incorrect one. As shown in Fig. 5, above a certain value, larger $m_{b\ell}^2$ comes often from the incorrect combination. To improve the purity of pairing, the events that have maximum $m_{b\ell}^2$ larger than a certain cut value are selected. A larger cut value improves the purity at the cost of reduced efficiency. In order to find the best cut value (leading to maximum sensitivity, $\epsilon(2P - 1)^2$) on $m_{b\ell}^{max}$, one can scan through various maximum invariant mass cut values and select the events having maximum invariant mass larger than the cut. The efficiency and purity are calculated for each cut value.

Kinematic method: the kinematic method is a variation of the method used in the top mass analysis in the dilepton channel. This method is based on resolving the full energy-momentum conservation equation set for all the particles in the final states. By a process of eliminating variables one is left with a 4th-order polynomial equation. Therefore up to 4 real solutions are possible. The CDF collaboration uses a numerical method to solve equations

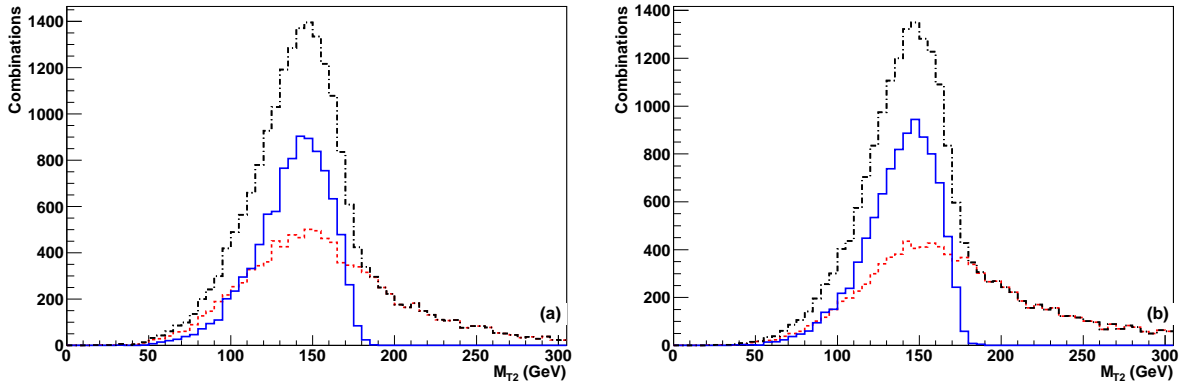


Figure 4: The M_{T2} distributions of the b - l combinations in the final state of the $t\bar{t}$ pair production at the Tevatron (a) and the LHC (b). They show the clear kinematic edges at m_{top} . The distribution of correct combinations is shown in blue (solid), while the incorrect one is in red (dotted) and all combinations are in black (dot-dashed).

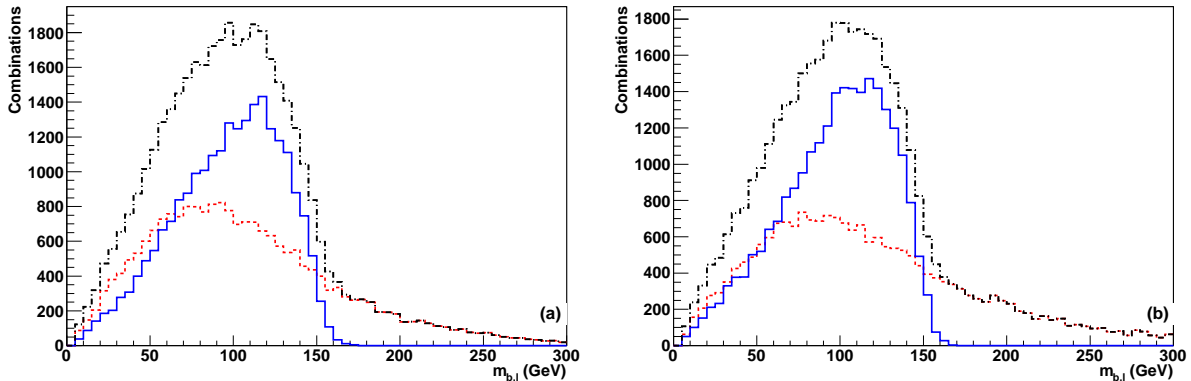


Figure 5: The invariant mass ($m_{b\ell}$) distributions of the b - l combinations in the final state of the $t\bar{t}$ pair production at the Tevatron (a) and the LHC (b). They show the clear kinematic edges at $\sqrt{m_{top}^2 - m_W^2}$.

and look for up to two solutions. If there are two solutions found, they choose the one having smaller $m_{t\bar{t}}$. A variation of this method has been used in studies of spin correlation of the $t\bar{t}$ system [35]. The kinematic method has slightly higher efficiency than the $m_{b\ell}^{max}$ method but its purity is significantly lower [29]. Performance of the neutrino phi weighting method is similar to the kinematic method [29]. The matrix element method can be also used but we do not find any comments on the pairing purity in the literature.

As a comparison with our method, we have considered the $m_{b\ell}^{max}$ method (denoted as $(m_{b\ell}, \text{none})$ in Figs. 6 and 7, and Tables 9 and 10) used by the CDF collaboration. Fig.

Number of passed combinations	Number of events	Number of events with correct combinations
0	248	–
1	5173	4908
2	4575	4416

Table 7: Results broken down by number of combinations passing the both the invariant mass and M_{T2} cuts for events at the 7 TeV LHC. By selecting events with only one event passing, an efficiency of 51.7% with a purity of 94.9% is obtained.

Number of passed combinations	Number of events	Number of events with correct combinations
0	230	–
1	3990	3665
2	5778	5580

Table 8: The same as Table 7 but at the Tevatron. The corresponding efficiency and purity are 39.9% and 91.9%.

6 shows the purity-efficiency relation with the sensitivity at the Tevatron (in (a)) and the LHC (in (b)). This one-dimensional relation is due to a degree of freedom in choosing the invariant mass cut. The original CDF method is denoted as $(m_{b\ell}, \text{none})$ (solid, red) while (M_{T2}, none) (dashed, black) represent the same scheme with $m_{b\ell}$ replaced by M_{T2} . At the Tevatron when a cut of $m_{b\ell} > 151$ GeV is made, the maximum sensitivity is obtained and this method results in an efficiency of 37.2% and a purity of 96.3% for top quark production. The corresponding cuts for $(m_{b\ell}, \text{none})$ are shown in Table 9. These are comparable to results obtained with our proposal. For the LHC, both purity and efficiency are higher (see Fig. 6(b) and Table 10).

While the initial requirement of only one combination passing the cuts for our method results in reasonable values for efficiency, we can still improve this by making use of the events in which both combinations pass the cuts (nearly 50 percent of the events for the LHC). It is possible to implement another reconstruction method on these events. One example would be to combine our method with the $m_{b\ell}^{max}$ method to improve the total number of events in which a good combination can be selected, while not causing too large of an adverse effect on the purity. In this case, however, we do not find a noticeable improvement over the original method.

Instead, we take a different approach to increase the event efficiency and purity. The CDF procedure cuts out events in which the combination with the highest $m_{b\ell}$ or M_{T2} is not over the cut value, thus giving a lower efficiency. We look at those events and apply a second cut on the variable not used in the first case, thus applying the method with M_{T2} for events not passing the $m_{b\ell}$ selection, $(m_{b\ell}, M_{T2})$, and vice versa, $(M_{T2}, m_{b\ell})$. We find that the M_{T2} and invariant mass together with the CDF scheme lead to much better efficiency and purity than those obtained with one of them only. Fig. 7 shows contours of the efficiency

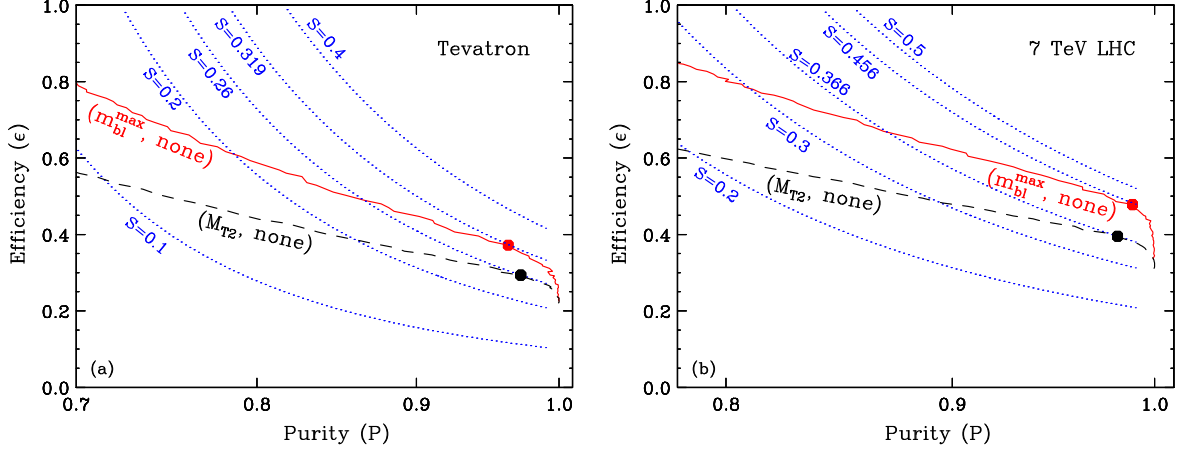


Figure 6: The efficiency, purity and sensitivity using the CDF method at the Tevatron (a) and the LHC (b). The original CDF method is denoted as (m_{bl}, none) (solid, red) while (M_{T2}, none) (dashed, black) represent the same scheme with m_{bl} replaced by M_{T2} . The contours of constant sensitivity are shown in dotted (blue) curves. The dots represent the efficiency and purity that results in the maximum sensitivity, and the corresponding cuts are shown in Tables 9 and 10.

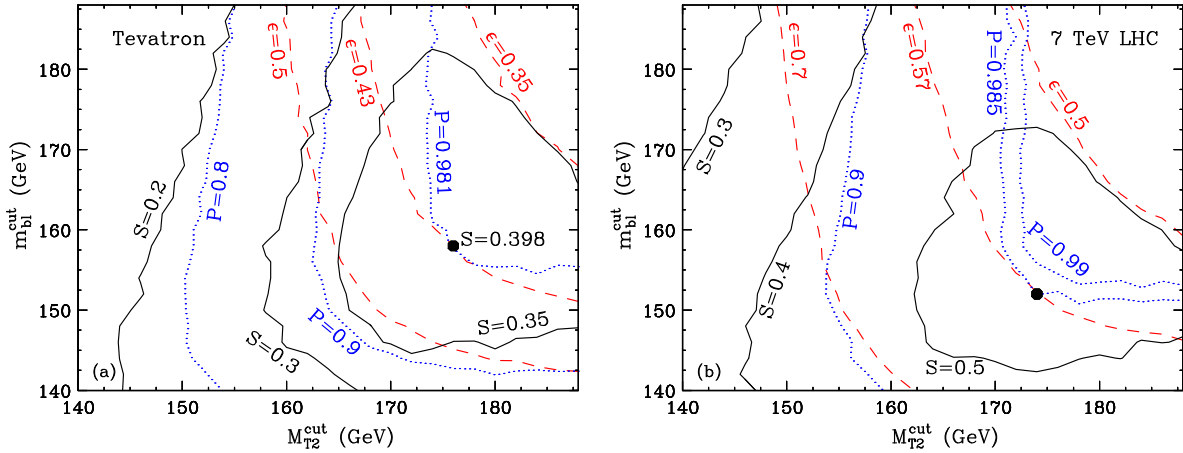


Figure 7: Contours of the efficiency (red, dashed), purity (blue, dotted) and sensitivity (black, solid) in the $M_{T2}-m_{bl}$ plane at the Tevatron (a) and the LHC (b). The dots represent the efficiency and purity that results in the maximum sensitivity. The corresponding cuts are shown in Tables 9 and 10.

(red, dashed), purity (blue, dotted) and sensitivity (black, solid) in the $M_{T2}-m_{bl}$ plane at the Tevatron (a) and the LHC (b). The cuts that correspond to the maximum sensitivity are shown in Table 10. Similar results are obtained for both (m_{bl}, M_{T2}) and (M_{T2}, m_{bl}) cases, and this shows the order of the two cuts is not crucial. With both kinematic cuts, we improve the efficiency by 20% while keeping the purity at the same level or slightly higher.

While in this section we have discussed the combinatorial ambiguity in the $b-\ell$ pairings

cut	cut value (GeV)	efficiency (ϵ)	purity (P)	sensitivity (S)
$(m_{b\ell}, \text{none})$	(151, none)	0.372	0.963	0.319
(M_{T2}, none)	(174, none)	0.294	0.972	0.261
$(m_{b\ell}, M_{T2})$	(158, 176)	0.426	0.981	0.398
$(M_{T2}, m_{b\ell})$	(175, 155)	0.442	0.971	0.392

Table 9: Results at the Tevatron for invariant mass cut, M_{T2} cut and the hybrid, following CDF scheme. The sensitivity is defined as $S = \epsilon(2P - 1)^2$.

cut	cut value (GeV)	efficiency (ϵ)	purity (P)	sensitivity (S)
$(m_{b\ell}, \text{none})$	(152, none)	0.478	0.988	0.456
(M_{T2}, none)	(172, none)	0.395	0.981	0.366
$(m_{b\ell}, M_{T2})$	(152, 174)	0.574	0.985	0.539
$(M_{T2}, m_{b\ell})$	(175, 155)	0.557	0.989	0.533

Table 10: The same as Table 9 but for the LHC.

in the dilepton channel, the same method can be used in principle in the semi-leptonic channel as well. In the latter case, often a χ^2 (or a likelihood function) is defined with mass-shell constraints of the top quark and the W boson on the both hadronic and leptonic sides, assuming the missing transverse momentum is solely due to the neutrino from the W decay. In the procedure, from the on-shell condition of the leptonic W , an additional two-fold ambiguity in sign for the z -component (along the beam direction) of the neutrino momentum is necessarily introduced. The correct combination and sign are determined by minimizing the χ^2 (or maximizing the likelihood function). The kinematic variables such as M_{T2} and invariant mass should be able to help to increase the probability of finding the correct combination, when they are properly included in the χ^2 or the likelihood functions.

We have assumed both b -jets are tagged but the proposed method here should apply in the final state with one b -tagged jet as well as in the dilepton channel with no b -tagged jets. In these cases, the candidates for the b -jet can be determined by different selection criteria. For instance, in the final state with one b -tagged jet, the hardest remaining jet could be a good candidate for the other b -jet while for the final state with no b -tagged jets, the two hardest jets are good choices. However the purity of the $t\bar{t}$ sample in the latter case will decrease significantly.

5. Summary and conclusions

The M_{T2} variable is originally introduced to measure masses of semi-invisibly decaying particles. It is the most natural extension to the transverse mass that was used for the W discovery and mass measurement. For the last few years, there have been many studies to determine masses, spins and couplings. Most of them utilize the kinematics of events with missing energy. The M_{T2} variable is especially useful for relatively short decay chains where a traditional invariant mass method is limited. The subsystem M_{T2} allows for measurement of

all masses in the decay chain, assuming combinatorial issues are sorted out. It is also shown that the M_{T2} variable shows an interesting kink structure due to the compositeness of the visible sector, the existence of ISR, or upstream transverse momentum from the heavier particle decays. It has been extended to include different mother/daughter particles masses. Finally it has been proposed as a potential solution for isolating ISR from signals with multiple jets.

In this paper we have investigated the feasibility of the use of M_{T2} to resolve combinatorial issues at hadron colliders. We concentrated on a 4-jets signal where 3 possible partitions exist. We have compared the performance of this method with the p_T versus invariant mass method and showed that efficiency increased up to a factor of 5 for the same purity of the sample. One of the advantages of the kinematic methods is that there is little dependence on the mass spectrum (model dependence), unlike a choice of p_T . We have found that our results for efficiency and purity remain similar for different choices of mass parameters. We showed that the kinematic variable suggested for mass determination is also useful for resolving combinatorial issues in signals, as well as for isolating ISR jets from signal jets.

A similar idea is applied to the $t\bar{t}$ dilepton system and we found that the obtained efficiency and purity are comparable to those using the current CDF method. A variation of their method with M_{T2} results in improvement of the efficiency by 20% at the Tevatron and 25% at the LHC, while the corresponding purity remains the same. It is desirable and important for experimental collaborations to revisit the method with a full detector simulation.

Acknowledgments

We thank Yen-Chu Chen for helpful discussion and providing relevant references regarding b - ℓ ambiguity in the $t\bar{t}$ production. This work is supported in part by US Department of Energy grants DE-FG02-04ER14308 and by National Science Foundation grants PHY-0653250. KK is supported partially by the National Science Foundation under Award No. EPS-0903806 and matching funds from the State of Kansas through the Kansas Technology Enterprise Corporation. KK acknowledges the hospitality of TASI-2011 at the University of Colorado, where some of this work was undertaken.

References

- [1] A. J. Barr, C. G. Lester, “A Review of the Mass Measurement Techniques proposed for the Large Hadron Collider,” *J. Phys. G* **G37**, 123001 (2010). [arXiv:1004.2732 [hep-ph]].
- [2] A. J. Barr, T. J. Khoo, P. Konar, K. Kong, C. G. Lester, K. T. Matchev, M. Park, “Guide to transverse projections and mass-constraining variables,” [arXiv:1105.2977 [hep-ph]].
- [3] A. J. Barr, T. J. Khoo, P. Konar, K. Kong, C. G. Lester, K. T. Matchev, M. Park, “A Storm in a ‘T’ Cup,” [arXiv:1108.5182 [hep-ph]].
- [4] I. Hinchliffe, F. E. Paige, M. D. Shapiro, J. Soderqvist and W. Yao, “Precision SUSY measurements at LHC,” *Phys. Rev. D* **55**, 5520 (1997). [arXiv:hep-ph/9610544].

- [5] N. Ozturk [ATLAS Collaboration], “SUSY Parameters Determination with ATLAS,” arXiv:0710.4546 [hep-ph].
- [6] B. Dutta, T. Kamon, N. Kolev, A. Krislock, “Bi-Event Subtraction Technique at Hadron Colliders,” [arXiv:1104.2508 [hep-ph]].
- [7] J. Alwall, A. Freitas, O. Mattelaer, “The Matrix Element Method and QCD Radiation,” Phys. Rev. **D83**, 074010 (2011). [arXiv:1010.2263 [hep-ph]].
- [8] J. Alwall, K. Hiramatsu, M. M. Nojiri *et al.*, “Novel reconstruction technique for New Physics processes with initial state radiation,” Phys. Rev. Lett. **103**, 151802 (2009). [arXiv:0905.1201 [hep-ph]].
- [9] M. M. Nojiri, K. Sakurai, “Controlling ISR in sparticle mass reconstruction,” Phys. Rev. **D82**, 115026 (2010). [arXiv:1008.1813 [hep-ph]].
- [10] P. Konar, K. Kong and K. T. Matchev, “ \sqrt{s}_{min} : A Global inclusive variable for determining the mass scale of new physics in events with missing energy at hadron colliders,” JHEP **0903**, 085 (2009). [arXiv:0812.1042 [hep-ph]].
- [11] P. Konar, K. Kong, K. T. Matchev, M. Park, “RECO level \sqrt{s}_{min} and subsystem \sqrt{s}_{min} : Improved global inclusive variables for measuring the new physics mass scale in E_T events at hadron colliders,” JHEP **1106**, 041 (2011). [arXiv:1006.0653 [hep-ph]].
- [12] D. Krohn, L. Randall, L. -T. Wang, “On the Feasibility and Utility of ISR Tagging,” [arXiv:1101.0810 [hep-ph]].
- [13] J. Alwall, S. Hoeche, F. Krauss *et al.*, “Comparative study of various algorithms for the merging of parton showers and matrix elements in hadronic collisions,” Eur. Phys. J. **C53**, 473-500 (2008). [arXiv:0706.2569 [hep-ph]].
- [14] T. Plehn, D. Rainwater, P. Z. Skands, “Squark and gluino production with jets,” Phys. Lett. **B645**, 217-221 (2007). [hep-ph/0510144].
- [15] J. Alwall, M. -P. Le, M. Lisanti *et al.*, “Model-Independent Jets plus Missing Energy Searches,” Phys. Rev. **D79**, 015005 (2009). [arXiv:0809.3264 [hep-ph]].
- [16] C. G. Lester and D. J. Summers, “Measuring masses of semi-invisibly decaying particles pair produced at hadron colliders,” Phys. Lett. B **463**, 99 (1999). [arXiv:hep-ph/9906349].
- [17] A. Barr, C. Lester and P. Stephens, “m(T2): The truth behind the glamour,” J. Phys. G **29**, 2343 (2003). [arXiv:hep-ph/0304226].
- [18] M. Burns, K. Kong, K. T. Matchev and M. Park, “Using Subsystem MT2 for Complete Mass Determinations in Decay Chains with Missing Energy at Hadron Colliders,” JHEP **0903**, 143 (2009). [arXiv:0810.5576 [hep-ph]].
- [19] K. T. Matchev, F. Moortgat, L. Pape, M. Park, “Precise reconstruction of sparticle masses without ambiguities,” JHEP **0908**, 104 (2009). [arXiv:0906.2417 [hep-ph]].
- [20] P. Konar, K. Kong, K. T. Matchev, M. Park, “Superpartner Mass Measurement Technique using 1D Orthogonal Decompositions of the Cambridge Transverse Mass Variable M_{T2} ,” Phys. Rev. Lett. **105**, 051802 (2010). [arXiv:0910.3679 [hep-ph]].
- [21] K. T. Matchev, M. Park, “A general method for determining the masses of semi-invisibly decaying particles at hadron colliders,” Phys. Rev. Lett. **107**, 061801 (2011). [arXiv:0910.1584 [hep-ph]].

- [22] A. Rajaraman, F. Yu, “A New Method for Resolving Combinatorial Ambiguities at Hadron Colliders,” *Phys. Lett.* **B700**, 126-132 (2011). [arXiv:1009.2751 [hep-ph]].
- [23] G. L. Bayatian *et al.* [CMS Collaboration], “CMS technical design report, volume II: Physics performance,” *J. Phys. G* **G34**, 995-1579 (2007).
- [24] J. Alwall, M. Herquet, F. Maltoni, O. Mattelaer, T. Stelzer, “MadGraph 5 : Going Beyond,” *JHEP* **1106**, 128 (2011). [arXiv:1106.0522 [hep-ph]].
- [25] E. Richter-Was [Atlas Collaboration], “Prospect for the Higgs searches with the ATLAS detector,” *Acta Phys. Polon.* **B40**, 1909-1930 (2009). [arXiv:0903.4198 [hep-ex]].
- [26] G. L. Bayatian *et al.* [CMS Collaboration], “CMS physics: Technical design report,”
- [27] A. J. Barr, B. Gripaios, C. G. Lester, “Transverse masses and kinematic constraints: from the boundary to the crease,” *JHEP* **0911**, 096 (2009). [arXiv:0908.3779 [hep-ph]].
- [28] P. Konar, K. Kong, K. T. Matchev and M. Park, “Dark Matter Particle Spectroscopy at the LHC: Generalizing MT2 to Asymmetric Event Topologies,” *JHEP* **1004**, 086 (2010). [arXiv:0911.4126 [hep-ph]].
- [29] Private communication with Yen-Chu Chen.
- [30] T. Sjostrand, S. Mrenna and P. Skands, “PYTHIA 6.4 Physics and Manual,” *JHEP* **0605**, 026 (2006). [arXiv:hep-ph/0603175].
- [31] J. Conway, <http://www.physics.ucdavis.edu/~conway/research/software/pgs/pgs4-general.htm>
- [32] N. Kidonakis, “Top quark cross sections and differential distributions,” [arXiv:1105.3481 [hep-ph]].
- [33] K. Melnikov and F. Petriello, <http://www.hep.wisc.edu/~frankjp/FEWZ.html>
- [34] J. Campbell and K. Ellis, <http://mcfm.fnal.gov/>
- [35] http://www-cdf.fnal.gov/physics/new/top/confNotes/cdf9824_spincorr2.8fb-1.pdf, CDF note 9824